

# A hierarchical analysis of the relationship between urban impervious surfaces and land surface temperatures: spatial scale dependence, temporal variations, and bioclimatic modulation

Qun Ma · Jianguo Wu · Chunyang He

Received: 30 November 2015 / Accepted: 27 February 2016 / Published online: 14 March 2016  
© Springer Science+Business Media Dordrecht 2016

## Abstract

**Context** Understanding how urban impervious surfaces (UIS) affect land surface temperatures (LST) on different scales in space and time is important for urban ecology and sustainability.

**Objectives** We examined how spatial scales, seasonal and diurnal variations, and bioclimatic settings affected the UIS–LST relationship in mainland China.

**Methods** We took a hierarchical approach explicitly considering three scales: the ecoregion, urban cluster, and urban core. The UIS–LST relationship was quantified with Pearson correlation using multiple remote sensing datasets.

**Results** In general, UIS and LST were positively correlated in summer daytime/nighttime and winter nighttime, but negatively in winter daytime. The strength of correlation increased from broad to fine scales. The mean  $R^2$  of winter nights at the urban core

scale (0.262) was 4.03 times as high as that at the ecoregion scale (0.065). The relationship showed large seasonal and diurnal variations: generally stronger in summer than in winter and stronger in nighttime than in daytime. At the urban core scale, the mean  $R^2$  of summer daytime (0.208) was 3.25 times as high as that of winter daytime (0.064), and the mean  $R^2$  of winter nighttime (0.262) was 4.10 times as high as that of winter daytime (0.064). Vegetation and climate substantially modified the relationship during summer daytime on the ecoregion scale.

**Conclusions** Our study provides new evidence that the UIS–LST relationship varies with spatial scales, diurnal/seasonal cycles, and bioclimatic context, with new insight into the cross-scale properties of the relationship. These findings have implications for mitigating urban heat island effects across scales in China and beyond.

---

**Electronic supplementary material** The online version of this article (doi:[10.1007/s10980-016-0356-z](https://doi.org/10.1007/s10980-016-0356-z)) contains supplementary material, which is available to authorized users.

---

Q. Ma · J. Wu · C. He (✉)  
Center for Human-Environment System Sustainability (CHESS), State Key Laboratory of Earth Surface Processes and Resource Ecology (ESPRE), Beijing Normal University, Beijing 100875, China  
e-mail: hcy@bnu.edu.cn

J. Wu  
School of Life Sciences and School of Sustainability, Arizona State University, Tempe, AZ 85287, USA

**Keywords** Urban impervious surfaces · Land surface temperatures · Urban heat islands · Urban landscape sustainability · China

## Introduction

The world has been urbanizing at an unprecedented rate since the 1950s, with more than 53 % of the global population now living in urban areas (Liu et al. 2014; Wu et al. 2014). Consequently, the global area of

urban impervious surfaces (UIS) has increased rapidly (Elvidge et al. 2007; Xian and Homer 2010). UIS refers to human-made land covers in urban areas through which water cannot penetrate, including rooftops, parking lots, roads, driveways, and sidewalks (Arnold and Gibbons 1996; Weng 2012; Ma et al. 2014). In 2010, the global UIS was about 595,971 km<sup>2</sup>, accounting for 0.45 % of the world's land area (Sutton et al. 2010; Liu et al. 2014). UIS eradicates previous vegetation, covers up soils, and profoundly modifies the local biophysical settings, resulting in myriad effects on biodiversity and ecosystem functions, hydrological and biogeochemical cycles, and local and regional climate. Thus, impervious surface coverage has been considered as “a key environmental indicator” (Arnold and Gibbons 1996).

The urban heat island (UHI) phenomenon is one of the best-documented UIS-related environmental problems (Oke 1982; Arnfield 2003; Voogt and Oke 2003; Buyantuyev and Wu 2010; Zhou et al. 2014a). UHI refers to the phenomenon that air and land surface temperatures (LST) are higher in an urban area than its surrounding rural area (Oke 1982; Arnfield 2003). In this study, we focused only on the surface UHI because it is related more directly to land surface characteristics (Gallo et al. 2002; Voogt and Oke 2003; Zhou et al. 2014b). Surface UHI occurs as a result of the replacement of vegetation by UIS, decreasing latent heat flux and increasing sensible heat flux and anthropogenic heat release (Yuan and Bauer 2007; Buyantuyev and Wu 2010). Increased land surface temperatures may increase energy use and water consumption, decrease air quality, alter biotic communities, and affect human health (Grimm et al. 2008; Wu 2014). Therefore, understanding the relationship between UIS and LST is important for understanding the interactions between climate change and UHI, and improving urban environmental sustainability (Wu 2013, 2014).

The relationship between UIS and LST has become a major research focus in urban studies during the past few decades, particularly in the context of climate change and urban environmental conditions (Zhou et al. 2004; Chen et al. 2006; Zhang et al. 2009a, b; Li et al. 2011; Luo and Li 2014; Zhou et al. 2014b; Kuang et al. 2015). Most of these studies have focused on LST, not UHI intensity (i.e., urban–rural temperature differences). The quantification of UHI is affected by

the delineation of “urban” and “rural” boundaries, whereas LST measurements can be made on the pixel level. Because most of these studies have focused on single cities and individual urban regions, a comparative and multi-scale understanding of the UIS–LST relationship is still lacking. Specifically, the spatial scale-dependence and seasonal and diurnal variations of the UIS–LST relationship over broad regions are not well understood, although relevant studies do exist (Zhang et al. 2009a; Imhoff et al. 2010; Zhang et al. 2010, 2012; Luo and Li 2014; Zhou et al. 2014b). Also, bioclimatic settings (associated with ecoregions and climatic regions), likely an important modulator of the surface UHI (Imhoff et al. 2010; Zhang et al. 2010, 2014; Bounoua et al. 2015), have not been adequately considered in the study of the UIS–LST relationship.

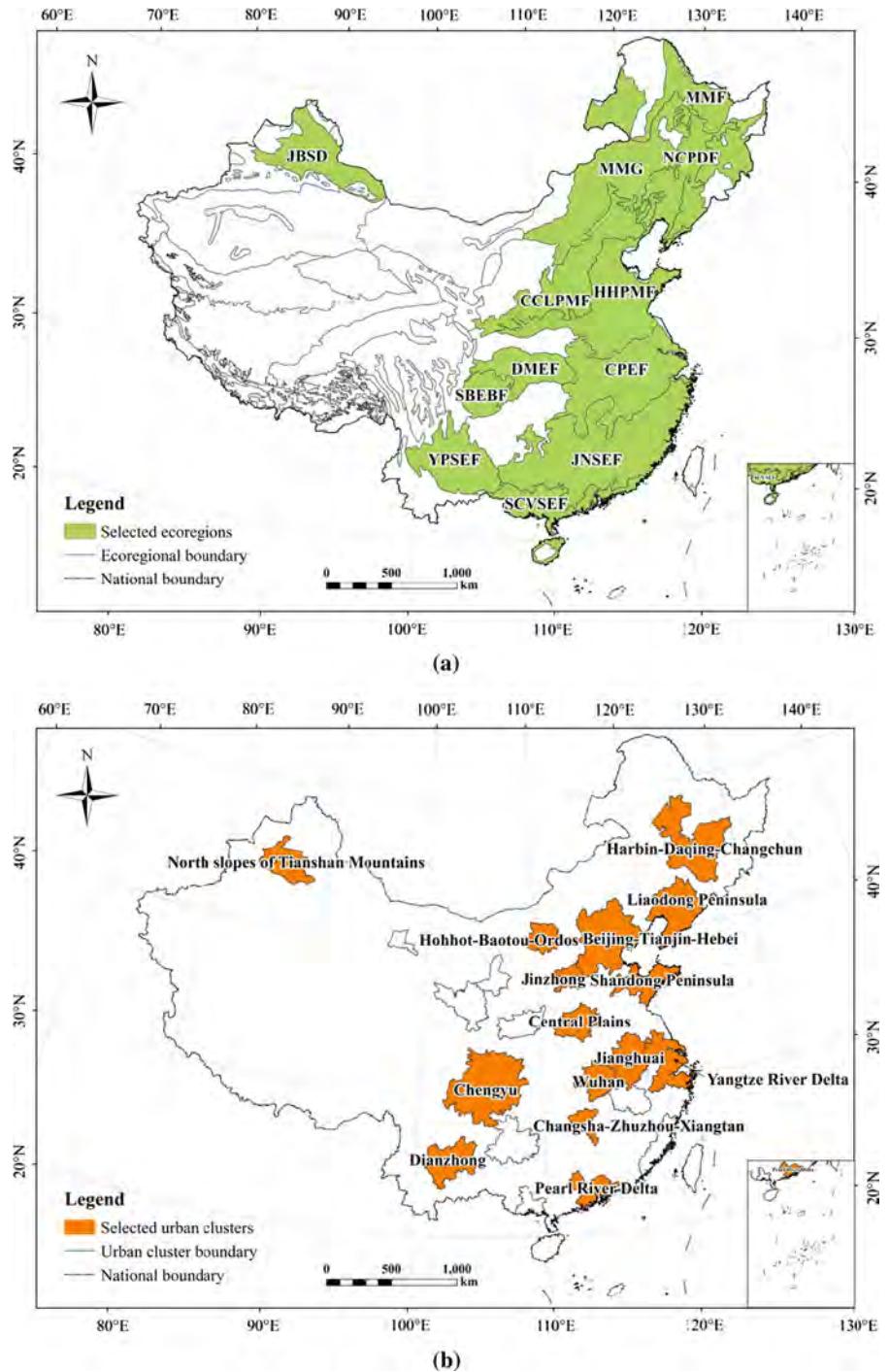
A substantial number of the recent UHI studies have come out of China because of its unprecedented speed and scale of urbanization in human history, as well as increasing concerns with urbanization-induced environmental problems (Wu et al. 2014). Since 1992, China's UIS area has been expanding at a rate of 6.54 % per year, which is probably the highest around the world (Ma et al. 2014). With a wide range of bioclimatic conditions and uneven urban growth rates across the country, China provides an ideal laboratory for studying how UIS affects LST and urban climate in general. Taking advantage of a comprehensive dataset of land covers and surface temperatures which covers the entire mainland China, our study was designed to address the following questions: (1) How does the UIS–LST relationship change from the local city to the ecoregion scale? (2) How does the UIS–LST relationship change diurnally and seasonally on different spatial scales? (3) How do vegetation and climate affect the UIS–LST relationship on different scales?

## Methods

### Study area and data acquisition

Our study area was mainland China, which did not include Taiwan and the islands in South China Sea (Fig. 1). We used five types of remote sensing data in our analysis: Moderate Resolution Imaging Spectroradiometer (MODIS)/Aqua 8-day LST composite data, nighttime light (NTL) data, MODIS 16-day

**Fig. 1** Locational maps of the study sites in mainland China on three spatial scales: **a** 12 ecoregions, **b** 15 urban clusters, and **c** 45 urban core areas. The 12 ecoregions are (1) Junggar Basin Semi-Desert (JBSD), (2) Manchurian Mixed Forests (MMF), (3) Northeast China Plain Deciduous Forests (NCPDF), (4) Mongolian-Manchurian Grassland (MMG), (5) Huang He Plain Mixed Forests (HHPMF), (6) Central China Loess Plateau Mixed Forests (CCLPMF), (7) Changjiang Plain Evergreen Forests (CPEF), (8) Daba Mountains Evergreen Forests (DMEF), (9) Sichuan Basin Evergreen Broadleaf Forests (SBEBF), (10) Jian Nan Subtropical Evergreen Forests (JNSEF), (11) Yunnan Plateau Subtropical Evergreen Forests (YPSEF), (12) South China–Vietnam Subtropical Evergreen Forests (SCVSEF)



NDVI composite data, high-resolution images available on Google Earth, and land use/cover data. The sources and relevant details of these data are described below.

The version 5 MODIS/Aqua 8-day LST composite data (MYD11A2) with a spatial resolution of  $1 \times 1$  km in 2009 were obtained from the National Aeronautics and Space Administration (NASA)/

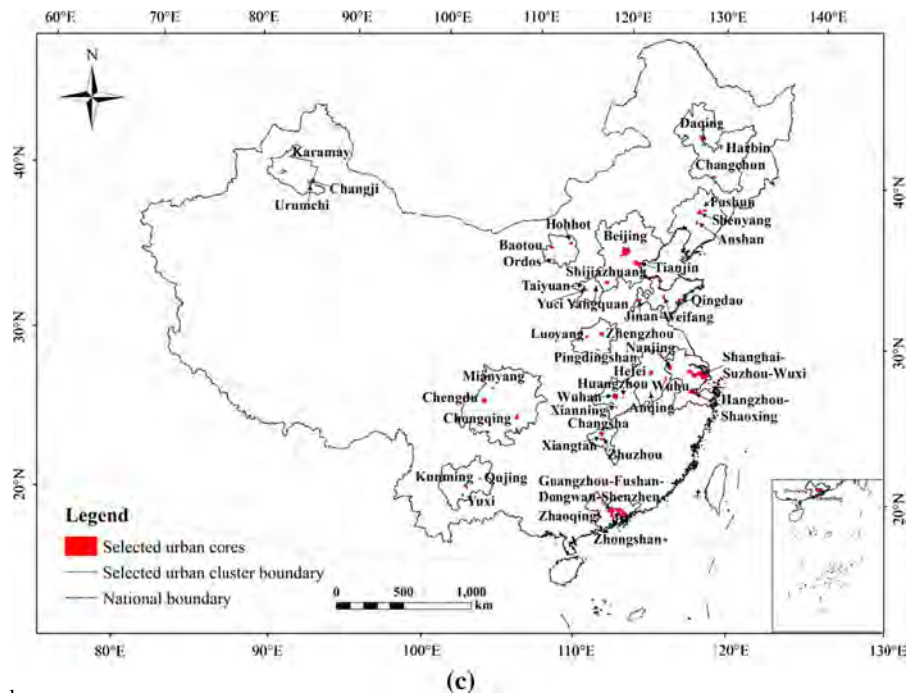


Fig. 1 continued

Goddard Space Flight Center (GSFC) (<http://adsweb.nascom.nasa.gov/data/search.html>). MYD11A2 LST data were retrieved from clear-sky (99 % confidence level) observations at 1:30 AM and 1:30 PM local solar times, using a generalized split-window algorithm (Wan and Dozier 1996). The data were average clear-sky LSTs over the period of 8 days (Wan 2007), with errors within 1 K in most tested cases (Wan 2008). The version 4 Defense Meteorological Satellite Program's Operational Linescan System (DMSP/OLS) NTL data in 2009 were acquired from the National Oceanic and Atmospheric Administration (NOAA)/National Geophysical Data Center (NGDC) (<http://ngdc.noaa.gov/eog/dmsp/downloadV4composites.html>). The NTL data were given in 30-arc-second grids. We projected the NTL data onto an Albers conical equal area projection and resampled the data to a pixel size of 1 km, based on a nearest neighbor resampling algorithm.

The version 4 MODIS/Terra 16-day NDVI composite data were obtained from NASA/GSFC (<http://adsweb.nascom.nasa.gov/data/search.html>) for the year of 2009, with a spatial resolution of  $1 \times 1$  km. We also took advantage of high-resolution images

(e.g., Aerial Imagery, QuickBird, and IKONOS) available on Google Earth, which contained rich spatial information on land covers with a spatial resolution of less than 5 m. National land use/cover datasets of China were provided by the data sharing infrastructure of the earth system science (<http://www.geodata.cn/Portal/index.jsp>). Monthly precipitation and temperature data in 2009 were obtained from the China Meteorological Data Sharing Service System (<http://cdc.nmic.cn/home.do>).

#### Selection of multiple spatial scales

To adequately address the problem of scale dependence of the UIS–LST relationship, we explicitly considered three spatial scales: the ecoregion, urban cluster (i.e., the agglomeration of closely connected cities), and urban core (i.e., the area with contiguous urbanized pixels expanding from the city center) (Fig. 1). The main justification for choosing these three scales is that most existing UHI-related studies have been carried out on these scales, and thus our results would be comparable to previous ones.

Although each of the three scales has been used in previous studies, our study is among the first to consider them simultaneously in a hierarchical manner.

To ensure enough data for adequately addressing the research questions without overburdening the analysis, we selected 12 of the 64 ecoregions in China classified by Olson et al. (2001), according to the following criteria: (1) the ecoregion is located within a major climate zone, (2) it includes the most rapidly urbanizing areas in that region during the recent decade, and (3) it contains a large enough number of UIS pixels for regression analysis (Fig. 1a). Then, 15 urban clusters were chosen from the 12 ecoregions, which included both national-level (e.g., Beijing-Tianjin-Hebei, Yangtze River Delta, and Pearl River Delta) and regional-level urban clusters (e.g., Hohhot-Baotou-Ordos, Jinzhong, and Dianzhong) (Fig. 1b). The map of urban clusters was created according to the criteria outlined in Fang et al. (2005) and Fang (2011), which included, among others, at least one megacity with a total population of larger than one million, an urbanization rate of above 50 %, and per capita GDP of greater than 3000 US dollars. Finally, within each urban cluster, we selected three urban cores of the largest prefecture-level cities, each of which was composed of contiguous urban pixels (Fig. 1c). The specific methods for delineating urban cores are described in the next section.

### Quantification of urban impervious surfaces

A number of remote sensing-based methods have been used to extract UIS (Lu et al. 2014). In this study, we used the method developed by Ma et al. (2014) to quantify UIS in mainland China because of its improved accuracy. Five steps were carried out to estimate the percent UIS value for each pixel in urban cores. First, a thresholding technique was adopted to extract urban cores, using the preprocessed NTL data and land use/cover data (Liu et al. 2012). The optimal threshold was determined when the urban cores extracted from the NTL data best matched the urban cores extracted from the land use/cover data in terms of the spatial extent. Second, we calculated Vegetation Adjusted NTL Urban Index (VANUI) in urban cores, with the following formula (Zhang et al. 2013):

$$VANUI = (1 - NDVI) * NTL_{nor} \quad (1)$$

where *NDVI* is the annual mean NDVI derived from MODIS, and  $NTL_{nor}$  is the normalized value of the preprocessed NTL data.  $NTL_{nor}$  was computed as:

$$NTL_{nor} = \frac{NTL - NTL_{min}}{NTL_{max} - NTL_{min}} \quad (2)$$

where  $NTL_{min}$  and  $NTL_{max}$  are the minimum and maximum values in the NTL data (0 and 63, respectively). Third, we randomly generated samples with a window size of  $1 \times 1$  km in urban cores and obtained their actual percent UIS values using Google Earth images. Fourth, we developed linear regression models using the VANUI values of samples as the independent variable, and the actual percent UIS values of samples as the dependent variable. Fifth, we applied the linear regression models and the VANUI values acquired from step 2 to estimate the percent UIS values in mainland China in 2009. To capture regional differences in geography and socioeconomic conditions, we divided China into eight regions and performed all the steps for each region (Ma et al. 2014). Our earlier accuracy assessment showed that this method had a much higher accuracy than other existing methods using NTL data: the average root-mean-square error (RMSE) was 0.128, mean absolute error (MAE) was 0.105, systematic error (SE) was -0.008, and correlation coefficient (R) was 0.846 (Ma et al. 2014).

### Land surface temperatures and bioclimatic data

We calculated the seasonal (i.e., summer and winter) average LST values for daytime (1:30 PM) and nighttime (1:30 AM), respectively. Summer includes June, July, and August, and winter includes December, January, and February (Imhoff et al. 2010; Zhou et al. 2014a). Taking seasonal mean LST for both daytime and nighttime can reduce the LST data sensitivity to environmental fluctuations (e.g., weather conditions).

NDVI, precipitation, and temperature data were used to investigate how the UIS-LST relationship would change with bioclimatic context. Average NDVI data in summer and winter were calculated for all urban core pixels in each region on different spatial scales to reflect the ecological context. Average precipitation and temperature data for both seasons were obtained from the meteorological stations

located within urban cores in each region to reflect the climatic background (Zhou et al. 2014a). There were 193 meteorological stations in urban core areas at the ecoregion scale, 107 at the urban cluster scale, and 37 at the urban core scale.

### Data analysis

Among all existing studies of the UIS-LST relationship, linear regression has been the most commonly used method (Yuan and Bauer 2007; Imhoff et al. 2010; Zhang et al. 2010), but other methods such as exponential or logarithmic regressions have also been used (Xu 2010; Myint et al. 2013). In this study, we compared four models (i.e., linear, exponential, logarithmic, and power models) based on the values of Akaike's information criterion (AIC) and coefficient of determination ( $R^2$ ) to determine the best model to quantify the UIS-LST relationship. The best model is the one with the lowest value of AIC and the highest value of  $R^2$  (Akaike 1978; Zhou et al. 2014b). In our study, the linear regression model turned out to be superior to other models at all three spatial scales. Thus, we conducted linear regression to quantify the relationship between UIS and LST, using the values of both variables for all urban core pixels in each region on different scales. All statistical analyses were performed with SPSS 16.0 (SPSS Inc.).

## Results

### UIS-LST relationship at the ecoregion scale

At the ecoregion scale, UIS and LST were significantly correlated for summer and winter as well as for day and night, and the correlation was positive in summer daytime/nighttime and winter nighttime, and negative in winter daytime (Fig. 2a–d; Table S1). Nearly all the ecoregions had a positive Pearson correlation coefficient in summer days/nights and winter nights (Fig. 3a). By contrast, half of the ecoregions had a negative Pearson correlation coefficient in winter days, with the average value of  $-0.19$  (Fig. 3a; Table S1). In general, the UIS–LST relationship at the ecoregion scale was stronger in summer than in winter, and stronger in daytime than in

nighttime for summer but weaker in daytime than in nighttime for winter (Figs. 3a and 4; Table S1). In other words, the relationship differed both seasonally and diurnally. Most of the Pearson correlation coefficients were larger than 0.30 in summer and smaller than 0.20 in winter (Fig. 3a; Table S1). During summer, the mean  $R^2$  of daytime was nearly twice that of nighttime, but the mean  $R^2$  of nighttime was about 2 times as high as that of daytime during winter (Fig. 4). As noted later, this result of higher averaged  $R^2$  in summer days than summer nights was not obtained on the other two scales.

The  $R^2$  values of the UIS-LST relationship varied substantially among ecoregions, without a clear trend in space except for summer daytime (Fig. 5a–d). The  $R^2$  values for summer daytime had a declining trend from high to low latitudes (Fig. 5a). Particularly, JBSD exhibited the largest  $R^2$  value of 0.42 during summer daytime (Fig. 5a; Table S1). By contrast, the summer daytime  $R^2$  values of ecoregions in southern China (e.g., CPEF, DMEF, JNSEF, and SCVSEF) were all smaller than 0.05 (Fig. 5a; Table S1).

### UIS–LST relationship at the urban cluster scale

At the urban cluster scale, UIS and LST were also significantly correlated, with pronounced seasonal and diurnal variations (Fig. 2e–h; Table S2). The relationship between the two variables was always positive except for winter daytime during which the relationship was negative or positive (Fig. 3b). The mean value of Pearson correlation coefficient was 0.35 for summer days, 0.44 for summer nights, and 0.32 for winter nights (Fig. 3b; Table S2). Three quarters of the ecoregions had a negative Pearson correlation coefficient for winter days, with a mean value of about  $-0.20$  (Fig. 3b; Table S2). Similar to the general pattern at the ecoregion scale, the UIS–LST relationship was stronger in summer than in winter, but the relationship was generally stronger in nighttime than in daytime for both seasons (Figs. 3b and 4; Table S2). For example, the mean  $R^2$  of summer daytime was almost 4 times that of winter daytime, and the mean  $R^2$  of winter nighttime was 3.2 times that of winter daytime (Fig. 4). The  $R^2$  values of different urban clusters also showed a high degree of spatial variability, without any clear trends in space for all time periods (Fig. 5e–h).

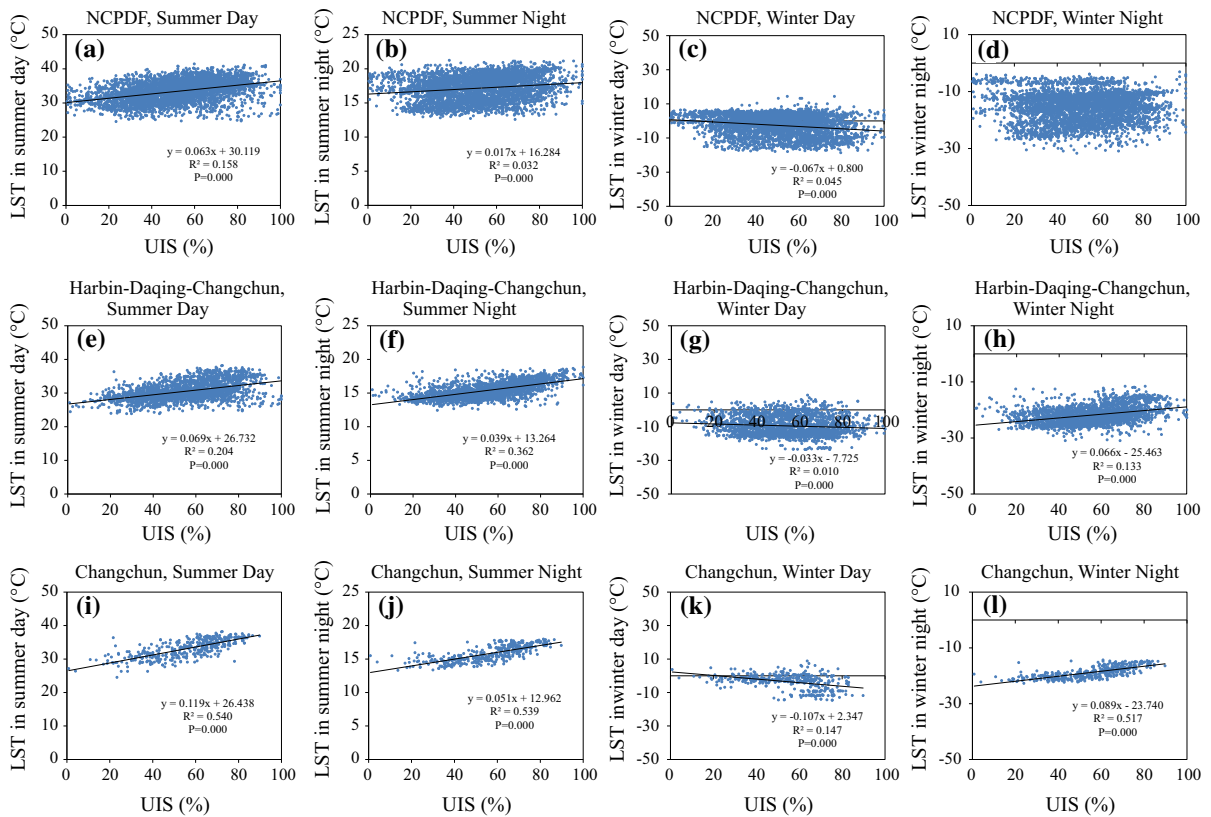


**Fig. 2** Examples of linear regressions between urban impervious surfaces (UIS, %) and land surface temperatures (LST, °C) on three spatially nested scales—ecoregion (Northeast China Plain Deciduous Forests, NCPDF), urban cluster (Harbin–

Daqing–Changchun), and urban core area (Changchun) and at four different times (summer day, summer night, winter day, and winter night)

UIS-LST relationship at the urban core scale

At the urban core scale, UIS and LST were again found significantly correlated with each other. The great majority of the Pearson correlation coefficients for summer daytime/nighttime and winter nighttime were positive, whereas most of those for winter daytime were negative (Figs. 2i–l and 3c; Table S3). The highest value of Pearson correlation coefficient was 0.80 for summer days, 0.75 for summer nights, and 0.80 for winter nights, while the lowest value of Pearson correlation coefficient was  $-0.54$  for winter days (Table S3). The  $R^2$  values of the relationship between UIS and LST varied seasonally and diurnally, and were generally higher in summer than in winter and higher in nighttime than in daytime (Fig. 4). The mean  $R^2$  value was 0.21 for summer days, 0.32 for summer nights, 0.06 for winter days, and 0.26 for winter nights (Fig. 4). So, the  $R^2$  values of the UIS-

LST relationship at the urban core scale were generally higher than those at the two larger scales, and they were also variable in space, without a clear trend (Fig. 5i–l).

Discussion

How does the UIS-LST relationship change with spatial scales?

Our results show that the relationship between urban impervious surfaces and land surface temperatures differed with spatial scales for the four different times of analysis—daytime, nighttime, summer, and winter, with mean  $R^2$  values increasing substantially from the ecoregion to the urban cluster and urban core scales (Fig. 4). For example, in both summer and winter, the mean  $R^2$  at the urban core scale was about 2 times that

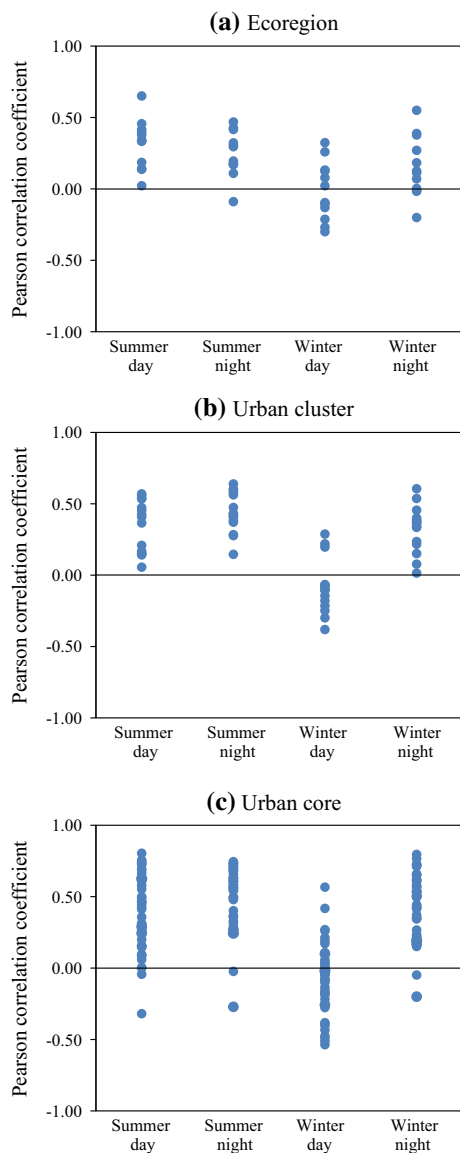


**Fig. 3** Pearson correlation coefficients for the UIS–LST relationship at four different times (summer day, summer night, winter day, and winter night) and on three different spatial scales of analysis (ecoregions, urban clusters, and urban core areas)

at the ecoregion scale for daytime and about 4 times for nighttime (Fig. 4). This means that the UIS–LST relationship became stronger on the average when the scale of analysis was focused more on the urban core.

The relatively weak relationship between UIS and LST on the broader scales (the urban cluster and the ecoregion) was mainly because the different bioclimatic conditions of ecoregions modified the effect of

UIS on LST. Imhoff et al. (2010) and Zhang et al. (2010) have shown that the regional-scale ecological context can act as an important modulator of the surface UHI. In our study, the mean UIS values at different spatial scales were similar (Fig. 6a), but the mean NDVI values decreased substantially from 0.45 at the ecoregion scale to 0.30 at the urban cluster scale and 0.28 at the urban core scale (Fig. 6b). Vegetation has a negative effect on LST via increasing evapotranspiration (Buyantuyev and Wu 2010; Imhoff et al. 2010; Zhou et al. 2014b). Thus, our results suggest that the relative impacts of vegetation on LST increase from the urban core to the urban cluster and ecoregion scales because of higher proportions of vegetation cover on the broader scales, which consequently weakens the UIS–LST relationship.

The range of  $R^2$  values of the relationship (i.e., the difference between the highest and the lowest  $R^2$  values) also increased with decreasing scales, indicating that the variability in the strength of the relationship was the highest on the urban core scale and the lowest at the ecoregion scale. For example, the range of  $R^2$  values for summer nights was 0.56 at the urban core scale, 0.39 at the urban cluster scale, and 0.21 at the ecoregion scale. The highest range of  $R^2$  values occurred at the urban core scale for summer days, with the largest  $R^2$  value of 0.65 and the smallest  $R^2$  value of 0.00 (Fig. 4). The large variability in the effect of UIS on LST on the urban core scale may be due to large variations in building materials as well as the composition and configuration of impervious surfaces (Zhou et al. 2011; Zhang et al. 2012; Zheng et al. 2014; Myint et al. 2013). For example, dark impervious surfaces (e.g., asphalt) can absorb and retain a high amount of heat, resulting in strong warming effects, whereas white and bright-colored impervious surfaces (e.g., high albedo concrete roads and white rooftops) can help reduce LST as they reflect most of the incoming solar radiation and maintain a low amount of heat (Georgescu et al. 2014). Also aggregated impervious surfaces and urban canyons have more intense warming effects than interspersed and flat urban morphological patterns (Oke 1981; Eliasson 1996; Chen et al. 2012).

The spatial pattern of  $R^2$  values also showed large variations across scales. At the ecoregion scale, the UIS–LST relationship changed with bioclimatic settings, with  $R^2$  decreasing from high to low latitudes for summer days (Fig. 5a). This latitudinal trend may be

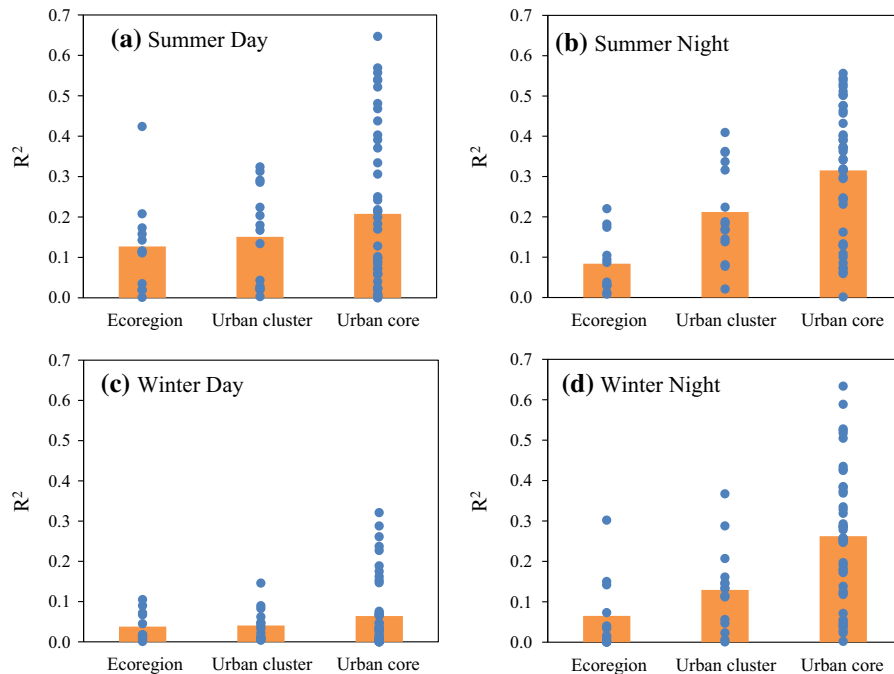


**Fig. 4** Comparison of the coefficient of determination ( $R^2$ ) for the UIS–LST relationship on three different spatial scales of analysis (ecoregions, urban clusters, and urban core areas) and at

four different times (summer day, summer night, winter day, and winter night). The *solid bars* in each plot denote the means of  $R^2$

attributable to directional changes in temperature, precipitation, and vegetation (Imhoff et al. 2010; Zhang et al. 2010). This trend was not observed at urban cluster and urban core scales (Fig. 5e–l), on which the spatial pattern of the UIS–LST relationship might be affected more strongly by other biophysical and anthropogenic factors. For example, Zhou et al. (2014a) found that both white-sky albedo (i.e., bihemispherical reflectance) and anthropogenic heat emissions were strongly correlated with the surface UHI intensity in China’s 32 major cities, with white-sky albedo explaining 42 % of the variance in summer daytime and anthropogenic heat emissions accounting for 65 % of the variance in winter nighttime.

The relationship between  $R^2$  values at different times varied greatly with spatial scales as well (Fig. 7). At the ecoregion scale, no correlation was found between daytime  $R^2$  and nighttime  $R^2$  for summer and winter, or between summer  $R^2$  and winter  $R^2$  for daytime and nighttime (Fig. 7a–d). At the urban cluster scale, one significantly positive relationship was found between summer  $R^2$  and winter  $R^2$  in nighttime (Fig. 7h). At the urban core scale, however, all the relationships between  $R^2$  values at different

times were significantly positively correlated (Fig. 7i–l). For example, summer nighttime  $R^2$  and winter nighttime  $R^2$  were highly correlated at the urban core scale, with a Pearson correlation coefficient of nearly 0.80 (Fig. 7l). These results suggest that at least some of the key factors influencing the UIS–LST relationship during daytime, nighttime, summer, and winter are common at the local urban scale, but not on broader scales.

How does the UIS–LST relationship change diurnally and seasonally?

Our study has shown that there was a significantly positive relationship between UIS and LST on three spatial scales and for all time periods but winter days (Fig. 3; Tables S1, S2, and S3). The positive relationship has been reported in previous studies (Yuan and Bauer 2007; Imhoff et al. 2010; Zhou et al. 2014a), which can be explained by the well-understood mechanisms of urban heat islands involving near-surface energy budgets (Buyantuyev and Wu 2010; Zhou et al. 2014b). The surface energy balance can be

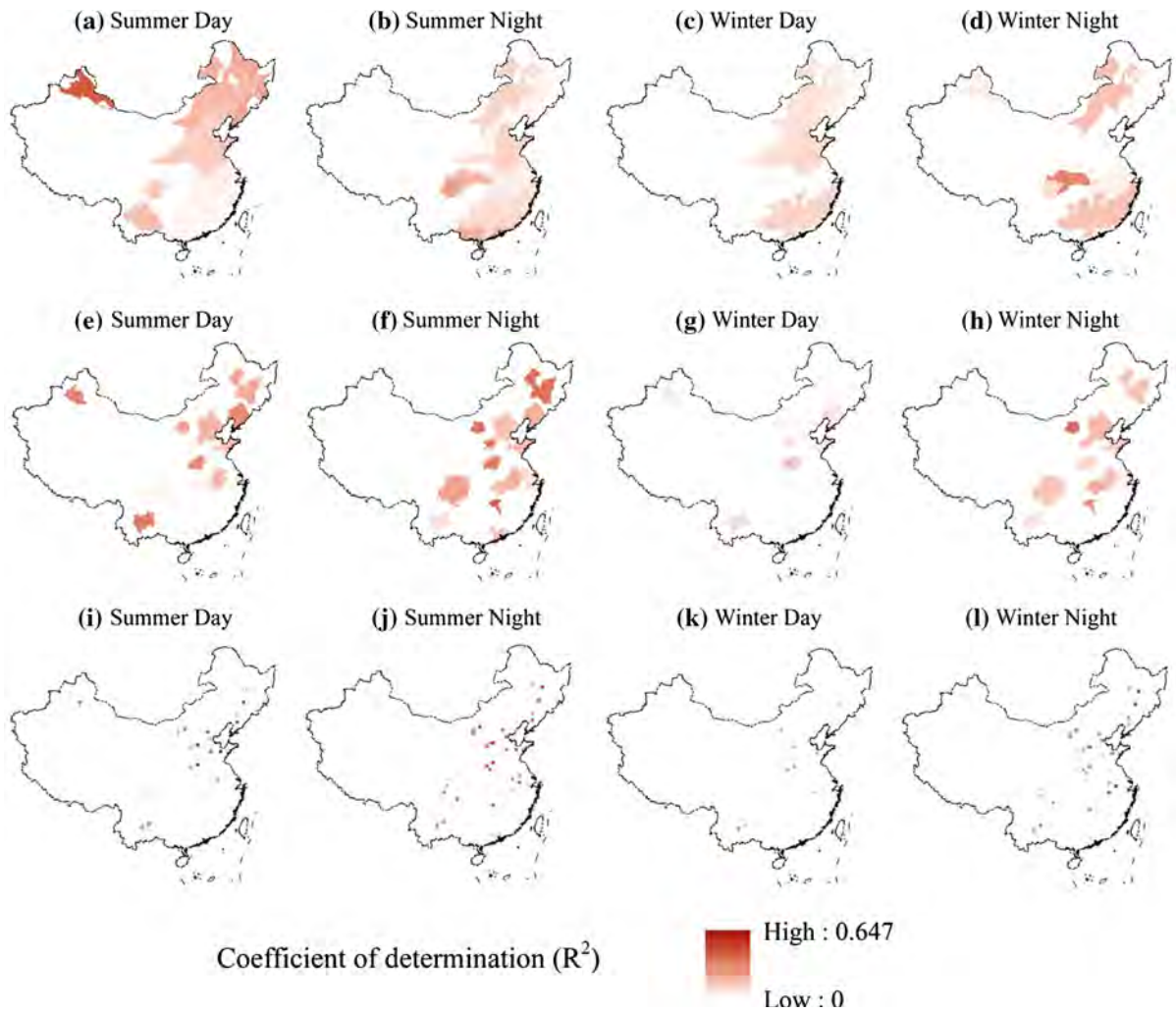


**Fig. 5** Spatial pattern of the  $R^2$  of the UIS–LST relationship on three spatial scales: ecoregions (a–d), urban clusters (e–h), and urban core areas (i–l) and at four different times: summer day, summer night, winter day, and winter night

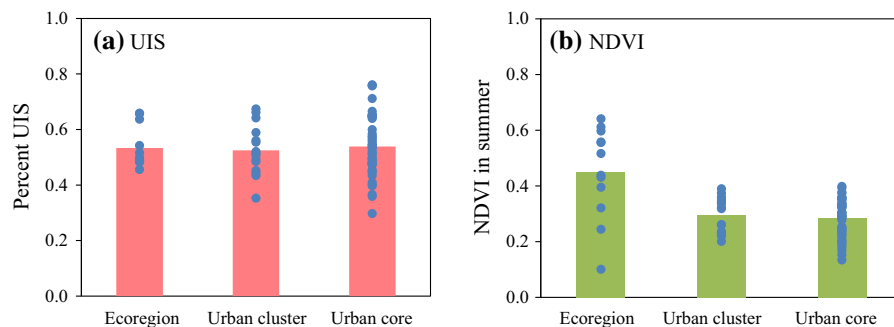


**Fig. 6** Percent UIS (a) and summer NDVI (b) on three different spatial scales (ecoregions, urban clusters, and urban core areas). The solid bars denote the mean values

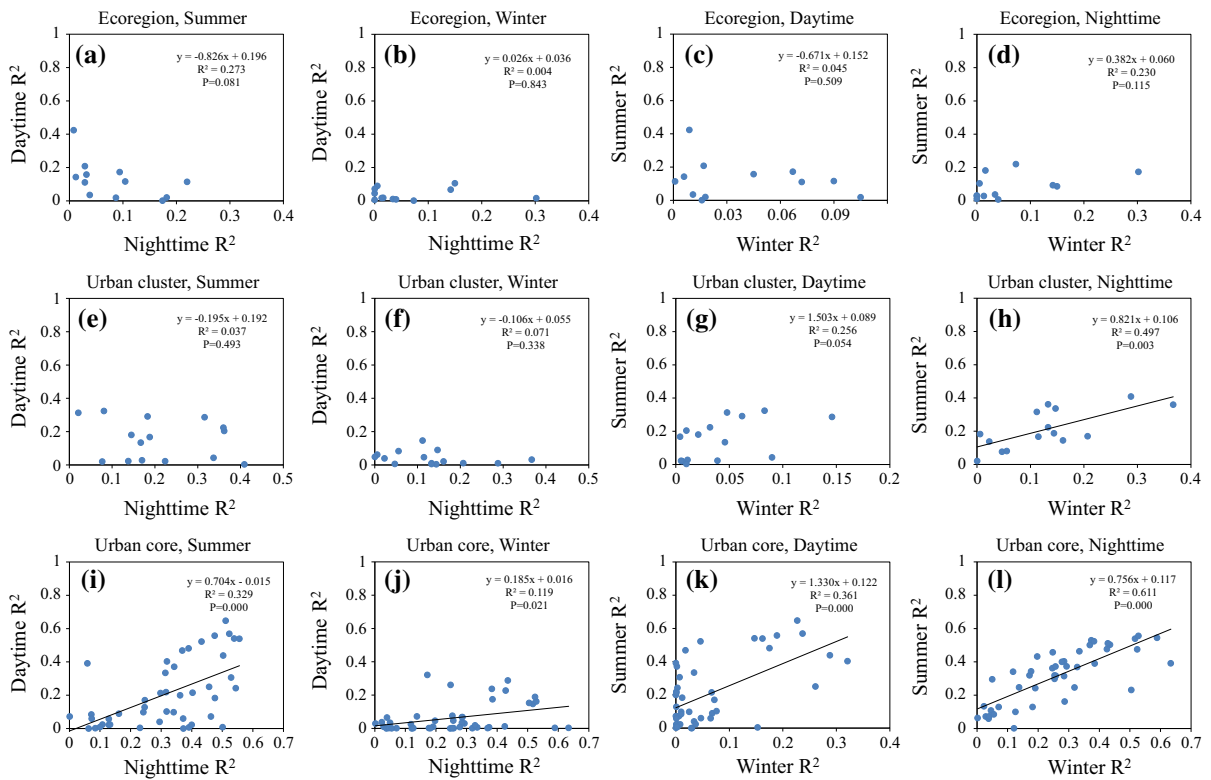


**Fig. 7** Relationships between the values of  $R^2$  of the UIS–LST relationship derived for daytime versus nighttime (a, b, e, f, i, and j), and for summer versus winter (c, d, g, h, k, and l) on three spatial scales—ecoregions, urban clusters, and urban core areas

written as:  $Net\ all - wave\ radiation + Anthropogenic\ heat\ releases = Latent\ heat\ flux + Sensible\ heat\ flux + Ground\ heat\ flux$  (Arnfield 2003; Clinton and Gong 2013; Zhou et al. 2014a). Increased UIS can reduce latent heat fluxes by decreasing evapotranspiration from soil-vegetation systems, and increase ground heat fluxes and sensible heat fluxes by absorbing more solar energy and subsequently releasing heat into the air. In addition, increases of UIS can also indirectly augment anthropogenic heat emissions by transportation, industry, and building infrastructure, all of which lead to increases in LST (Zhang et al. 2010; Zhou et al. 2014a; Kuang et al. 2015).

In contrast, UIS and LST were negatively correlated in winter daytime for most study sites on all three scales (Fig. 3; Tables S1, S2, and S3). This may be caused by multiple reasons. First, the high thermal inertia of building materials and shading by tall buildings may act somewhat like vegetation (Oke 1982; Buyantuyev and Wu 2010; Myint et al. 2013). Second, cold and dry soil surfaces without

vegetation during winter days may have a lower specific heat capacity than impervious surfaces (e.g., the specific heat values of dry soils, asphalt, and dry cement are 0.80, 0.92, and 1.55 kJ/Kg °C, respectively). Thus, during cold winter days the temperature of impervious surfaces tends to rise more slowly than non-impervious surfaces nearby, resulting in a “cooling effect”.

Previous studies reported that UIS and LST were significantly correlated with each other for all seasons (Yuan and Bauer 2007; Myint et al. 2013; Zhou et al. 2014b). Our study reveals large seasonal variability in the UIS–LST relationship on all three spatial scales, with higher mean  $R^2$  values in summer than in winter (Fig. 4). This implies that the variance of LST can be better explained by UIS in summer than in winter. This seasonal variability may be attributed to the differences in solar radiation and the length of the day between summer and winter. In summer, the solar radiation is higher and the day is longer than in winter, which allows UIS to absorb and store more sunlight,

thereby affecting LST more strongly (Buyantuyev and Wu 2010).

The UIS–LST relationship also had substantial diurnal differences on all three spatial scales, with stronger correlations in nighttime than in daytime, except for summer at the ecoregion scale (Fig. 4). This suggests that UIS has a larger effect on LST during nighttime than daytime. During daytime, vegetation can effectively decrease LST by increasing latent heat flux, and thus reduce the influence of UIS on LST. At night, the cooling effect of plants is minimal because of the lack of evapotranspiration (Buyantuyev and Wu 2010). Moreover, there is a high level of anthropogenic heat emissions at night, which can also increase the effect of UIS on LST.

How do vegetation and climate affect the UIS–LST relationship on different scales?

A number of studies have shown that vegetation and climate can influence the surface UHI (Imhoff et al. 2010; Zhang et al. 2010; Zhou et al. 2014a), but their effects on the UIS–LST relationship are yet to be understood. Our study has demonstrated that these two factors may affect the UIS–LST relationship substantially, but the effects vary greatly with spatial scales and time periods. Specifically, larger effects were found for summer days at the ecoregion scale (Fig. 8; Table S4), but little impact was observed for any time period at the other two scales (Figs. S1, S2, and S3). At the ecoregion scale, vegetation cover significantly weakened the UIS–LST relationship for summer days (Fig. 8a). More than 60 % of the variance in summer daytime  $R^2$  was explained by mean NDVI alone. This means that UIS tends to have a larger effect on LST in

ecoregions with lower vegetation cover. For example, JBSD had the largest  $R^2$  value of 0.42 during summer daytime, while having the lowest mean NDVI of 0.16 in summer (Fig. 8a). But vegetation had little impact on the UIS–LST relationship for summer nights and winter, mainly because of the absence or minimal amount of evapotranspiration during nighttime and winter (Yuan and Bauer 2007; Zhou et al. 2014a, 2014b) (Fig. S1a–c).

Similar to vegetation, climatic conditions (i.e., precipitation and temperature) were only found to affect the UIS–LST relationship during summer daytime and at the ecoregion scale (Figs. 8b–c and S1d–i). High precipitations and high temperatures tend to relax the relationship between UIS and LST (i.e., reducing its  $R^2$ ), with more than 58 % and 37 % of the variations in summer daytime  $R^2$  of the UIS–LST relationship explained by mean precipitation and temperature, respectively (Fig. 8b–c). This suggests that ecoregions situated in dry and cold climates generally have higher  $R^2$  values for summer days than those under humid and hot climates. Humid and hot regions often have much higher soil moistures which dampen the effect of UIS on LST (Zhou et al. 2014a). Latitudinal variations of climatic factors and vegetation (or NDVI) together seem to explain the general trend that the UIS–LST relationship weakens from north to south in China, as indicated by declining  $R^2$  (Fig. 5a).

At the urban cluster and urban core scales, the effects of vegetation and climate on the UIS–LST relationship were not detected (Figs. S2 and S3), probably because other factors at these finer scales played a more dominant role in determining the relationship. A number of environmental and

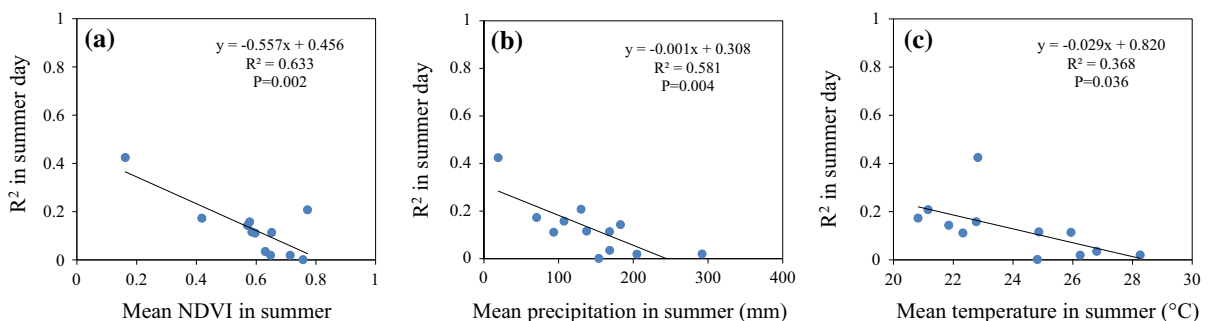


**Fig. 8** Linear regressions of  $R^2$  for summer daytime against **a** mean summer NDVI values, **b** mean summer precipitation (mm), and **c** mean summer temperature (°C) on the ecoregion scale

socioeconomic factors, such as landscape configuration, surface albedo, anthropogenic heat emissions, and city size in terms of urban population and urbanized land, have been shown to affect the magnitude and spatial pattern of surface UHIs (Tran et al. 2006; Jenerette et al. 2007; Buyantuyev and Wu 2010; Zhou et al. 2011; Clinton and Gong 2013; Zhou et al. 2014a). All of these factors may influence the UIS-LST relationship at the urban cluster and urban core scales, which demands further studies.

## Conclusions

Our study has demonstrated that both the strength and variability of the relationship between urban impervious surfaces and land surface temperatures tend to increase from broader regional scales to the local urban scale. The UIS–LST relationship also varies diurnally and seasonally, with a positive correlation for summer daytime/nighttime and winter nighttime and a negative correlation for winter daytime. The relationship is generally stronger in summer than in winter, as well as stronger in nighttime than in daytime. Bioclimatic conditions can substantially modulate the UIS–LST relationship for summer daytime across ecoregions, so that the relationship is stronger in dry and cold regions and weaker in wet and hot regions.

Although previous studies have shown that UIS is generally a good predictor of LST (Sheng et al. 2015; Zhang et al. 2012; Zhou et al. 2014b), our study reveals that UIS predicts LST primarily on the local urban scale. This suggests that the amount and configuration of UIS can be manipulated via landscape planning most effectively at local urban scales to mitigate urban heat island effects. Large variations in the strength of the UIS–LST relationship on the local urban scale further imply that this mitigation potential is quite substantial. In addition, our findings on the scale multiplicity, temporal variations, and context dependence of the UIS–LST relationship have important implications for better understanding the environmental impacts of urban impervious surfaces. One obvious lesson is that the results of single-scale, single-place, or single-time studies of UIS effects are partial or even misleading. This calls for multiscale, multi-seasonal, and

paired day-night studies in multiple regions. Thus, using urban impervious coverage as “a key environmental indicator” is promising, but can be quite complex.

**Acknowledgments** We thank Zhifeng Liu and Zexiang Sun for their assistance with data acquisition and processing. We also thank anonymous reviewers for their valuable comments. This research was supported in part by the National Basic Research Programs of China (Grant No. 2014CB954302 and 2014CB954303) and the National Natural Science Foundation of China (Grant No. 41321001).

## References

- Akaike H (1978) On the likelihood of a time series model. *Statistician* 217–235
- Arnfield AJ (2003) Two decades of urban climate research: a review of turbulence, exchanges of energy and water, and the urban heat island. *Int J Climatol* 23(1):1–26
- Arnold CL, Gibbons CJ (1996) Impervious surface coverage—the emergence of a key environmental indicator. *J Am Plann Assoc* 62(2):243–258
- Bounoua L, Zhang P, Mostovoy G, Thome K, Masek J, Imhoff M, Shepherd M, Quattrochi D, Santanello J, Silva J, Wolfe R (2015) Impact of urbanization on US surface climate. *Environ Res Lett* 10(8):084010
- Buyantuyev A, Wu J (2010) Urban heat islands and landscape heterogeneity: linking spatiotemporal variations in surface temperatures to land-cover and socioeconomic patterns. *Landscape Ecol* 25(1):17–33
- Chen L, Ng E, An X, Ren C, Lee M, Wang U, He Z (2012) Sky view factor analysis of street canyons and its implications for daytime intra-urban air temperature differentials in high-rise, high-density urban areas of Hong Kong: a GIS-based simulation approach. *Int J Climatol* 32(1):121–136
- Chen X, Zhao H, Li P, Yin Z (2006) Remote sensing image-based analysis of the relationship between urban heat island and land use/cover changes. *Remote Sens Environ* 104(2):133–146
- Clinton N, Gong P (2013) MODIS detected surface urban heat islands and sinks: global locations and controls. *Remote Sens Environ* 134:294–304
- Eliasson I (1996) Intra-urban nocturnal temperature differences: a multivariate approach. *Clim Res* 7:21–30
- Elvidge CD, Tuttle BT, Sutton PC, Baugh KE, Howard AT, Milesi C, Bhaduri B, Nemani R (2007) Global distribution and density of constructed impervious surfaces. *Sensors* 7(9):1962–1979
- Fang C (2011) New structure and new trend of formation and development of urban agglomerations in China. *Sci Geogr Sin* 31(9):1025–1034
- Fang C, Song J, Zhang Q, Li M (2005) The formation, development and spatial heterogeneity patterns for the structures system of urban agglomerations in China. *Acta Geogr Sin* 60(5):827–840

- Gallo KP, Adegoke JO, Owen TW, Elvidge CD (2002) Satellite-based detection of global urban heat-island temperature influence. *J Geophys Res* 107(D24):1–16
- Georgescu M, Morefield PE, Bierwagen BG, Weaver CP (2014) Urban adaptation can roll back warming of emerging megapolitan regions. *Proc Natl Acad Sci* 111(8):2909–2914
- Grimm NB, Faeth SH, Golubiewski NE, Redman CL, Wu J, Bai X, Briggs JM (2008) Global change and the ecology of cities. *Science* 319(5864):756–760
- Imhoff ML, Zhang P, Wolfe RE, Bounoua L (2010) Remote sensing of the urban heat island effect across biomes in the continental USA. *Remote Sens Environ* 114(3):504–513
- Jenerette GD, Harlan SL, Brazel A, Jones N, Larsen L, Stefanov WL (2007) Regional relationships between surface temperature, vegetation, and human settlement in a rapidly urbanizing ecosystem. *Landscape Ecol* 22(3):353–365
- Kuang W, Liu Y, Dou Y, Chi W, Chen G, Gao C, Yang T, Liu J, Zhang R (2015) What are hot and what are not in an urban landscape: quantifying and explaining the land surface temperature pattern in Beijing, China. *Landscape Ecol* 30(2):357–373
- Li J, Song C, Cao L, Zhu F, Meng X, Wu J (2011) Impacts of landscape structure on surface urban heat islands: a case study of Shanghai, China. *Remote Sens Environ* 115(12):3249–3263
- Liu Z, He C, Zhang Q, Huang Q, Yang Y (2012) Extracting the dynamics of urban expansion in China using DMSP-OLS nighttime light data from 1992 to 2008. *Landsc Urban Plan* 106(1):62–72
- Liu Z, He C, Zhou Y, Wu J (2014) How much of the world's land has been urbanized, really? A hierarchical framework for avoiding confusion. *Landscape Ecol* 29(5):763–771
- Lu DS, Li GY, Kuang WH, Moran E (2014) Methods to extract impervious surface areas from satellite images. *Int J Digit Earth* 7(2):93–112
- Luo X, Li W (2014) Scale effect analysis of the relationships between urban heat island and impact factors: case study in Chongqing. *J Appl Remote Sens* 8(1):1–13
- Ma Q, He C, Wu J, Liu Z, Zhang Q, Sun Z (2014) Quantifying spatiotemporal patterns of urban impervious surfaces in China: an improved assessment using nighttime light data. *Landsc Urban Plan* 130:36–49
- Myint SW, Wentz EA, Brazel AJ, Quattrochi DA (2013) The impact of distinct anthropogenic and vegetation features on urban warming. *Landscape Ecol* 28(5):959–978
- Oke TR (1981) Canyon geometry and the nocturnal urban heat island: comparison of scale model and field observations. *J Climatol* 1(3):237–254
- Oke TR (1982) The energetic basis of the urban heat island. *Q J R Meteorol Soc* 108(455):1–24
- Olson DM, Dinerstein E, Wikramanayake ED, Burgess ND, Powell GV, Underwood EC, D'Amico JA, Itoua I, Strand HE, Morrison JC, Loucks CJ (2001) Terrestrial ecoregions of the world: a new map of life on earth a new global map of terrestrial ecoregions provides an innovative tool for conserving biodiversity. *Bioscience* 51(11):933–938
- Sheng L, Lu D, Huang J (2015) Impacts of land-cover types on an urban heat island in Hangzhou, China. *Int J Remote Sens* 36(6):1584–1603
- Sutton PC, Elvidge CD, Tuttle BT, Ziskin D (2010) A 2010 mapping of the constructed surface area density for S.E. Asia—preliminary results. Proceedings of the 30th Asia-Pacific Advanced Network Meeting:182–190
- Tran H, Uchiyama D, Ochi S, Yasuoka Y (2006) Assessment with satellite data of the urban heat island effects in Asian mega cities. *Int J Appl Earth Obs Geoinf* 8(1):34–48
- Voogt JA, Oke TR (2003) Thermal remote sensing of urban climates. *Remote Sens Environ* 86(3):370–384
- Wan Z (2007) Collection-5 MODIS land surface temperature products users' guide. ICESSE, University of California, Santa Barbara
- Wan Z (2008) New refinements and validation of the MODIS land-surface temperature/emissivity products. *Remote Sens Environ* 112(1):59–74
- Wan Z, Dozier J (1996) A generalized split-window algorithm for retrieving land-surface temperature from space. *IEEE Trans Geosci Remote Sens* 34(4):892–905
- Weng Q (2012) Remote sensing of impervious surfaces in the urban areas: requirements, methods, and trends. *Remote Sens Environ* 117:34–49
- Wu J (2013) Landscape sustainability science: ecosystem services and human well-being in changing landscapes. *Landscape Ecol* 28(6):999–1023
- Wu J (2014) Urban ecology and sustainability: the state-of-the-science and future directions. *Landsc Urban Plan* 125:209–221
- Wu J, Xiang W-N, Zhao J (2014) Urban ecology in China: historical developments and future directions. *Landsc Urban Plan* 125:222–233
- Xian G, Homer C (2010) Updating the 2001 national land cover database impervious surface products to 2006 using landsat imagery change detection methods. *Remote Sens Environ* 114(8):1676–1686
- Xu H (2010) Analysis of impervious surface and its impact on urban heat environment using the normalized difference impervious surface index (NDISI). *Photogramm Eng Remote Sens* 76(5):557–565
- Yuan F, Bauer ME (2007) Comparison of impervious surface area and normalized difference vegetation index as indicators of surface urban heat island effects in landsat imagery. *Remote Sens Environ* 106(3):375–386
- Zhang P, Bounoua L, Imhoff ML, Wolfe RE, Thome K (2014) Comparison of MODIS land surface temperature and air temperature over the continental USA meteorological stations. *Can J Remote Sens* 40(2):110–122
- Zhang P, Imhoff ML, Bounoua L, Wolfe RE (2012) Exploring the influence of impervious surface density and shape on urban heat islands in the northeast United States using MODIS and landsat. *Can J Remote Sens* 38(04):441–451
- Zhang P, Imhoff ML, Wolfe RE, Bounoua L (2010) Characterizing urban heat islands of global settlements using MODIS and nighttime lights products. *Can J Remote Sens* 36(3):185–196
- Zhang Q, Schaaf C, Seto KC (2013) The vegetation adjusted NTL urban index: a new approach to reduce saturation and increase variation in nighttime luminosity. *Remote Sens Environ* 129:32–41
- Zhang X, Zhong T, Wang K, Cheng Z (2009a) Scaling of impervious surface area and vegetation as indicators to

- urban land surface temperature using satellite data. *Int J Remote Sens* 30(4):841–859
- Zhang Y, Odeh IO, Han C (2009b) Bi-temporal characterization of land surface temperature in relation to impervious surface area, NDVI and NDBI, using a sub-pixel image analysis. *Int J Appl Earth Obs Geoinf* 11(4):256–264
- Zheng B, Myint SW, Fan C (2014) Spatial configuration of anthropogenic land cover impacts on urban warming. *Landsc Urban Plan* 130:104–111
- Zhou D, Zhao S, Liu S, Zhang L, Zhu C (2014a) Surface urban heat island in China's 32 major cities: spatial patterns and drivers. *Remote Sens Environ* 152:51–61
- Zhou L, Dickinson RE, Tian Y, Fang J, Li Q, Kaufmann RK, Tucker CJ, Myneni RB (2004) Evidence for a significant urbanization effect on climate in China. *Proc Natl Acad Sci USA* 101(26):9540–9544
- Zhou W, Huang G, Cadenasso ML (2011) Does spatial configuration matter? Understanding the effects of land cover pattern on land surface temperature in urban landscapes. *Landsc Urban Plan* 102(1):54–63
- Zhou W, Qian Y, Li X, Li W, Han L (2014b) Relationships between land cover and the surface urban heat island: seasonal variability and effects of spatial and thematic resolution of land cover data on predicting land surface temperatures. *Landsc Ecol* 29(1):153–167